International Journal of Control, Automation and Systems 15(4) (2017) 1720-1728
http://dx.doi.org/10.1007/s12555-017-0289-6
ISSN:1598-6446 eISSN:2005-4092
http://www.springer.com/12555

Wind Direction Prediction for Yaw Control of Wind Turbines

Dongran Song, Jian Yang*, Yao Liu, Mei Su, Anfeng Liu, and Young Hoon Joo*

Abstract: Depending on historical signals from wind direction sensors, conventional yaw control methods provide general performance and may be optimized by taking advantage of wind direction prediction. This paper presents two wind direction prediction methods based on time series models. The first method adopts a univariate ARIMA (auto-regressive integrated moving average) model, while the second one uses a hybrid model that integrates the ARIMA model into a Kalman Filter (KF). Since the predicted results are used to optimize yaw control of wind turbines, six prediction models are developed using three types of mean wind directions. Finally, industrial data is used to develop, validate and test the proposed models. From obtained results, it is shown that the hybrid models outperform other ones in terms of three performance indexes and different types of wind direction time series.

Keywords: ARIMA, Kalman filter wind turbine, wind direction prediction, yaw control.

1. INTRODUCTION

As the rapidest developing renewable energy, wind power generation has been impressive in recent years. The latest statistical data from Global Wind Energy Council [1] shows that, the global cumulative capacity of wind power has reached 486.7[GW] in 2016, with a newly added capacity of 54.6[GW] in 2016. In America of 2030, it is anticipated that more than 20% energy production will be provided by wind energy [2]. Meanwhile, Chinese government makes an energy plan [3] that non-fossil energy will rise to 15% and 20% in the national total primary energy consumption by 2020 and 2030, respectively. From these data, it is observed that wind energy has become an important portion of energy. Wind turbines (WTs) are the main equipment in charge of wind power capture and generation, thus it is important to optimize performance of WTs.

To ensure high performance while minimizing costs, optimal solutions have been developed constantly for WTs. Among various solutions, control technology plays an indispensable role that directly affects WTs' power production and their component loads [4]. For modern horizontal-axis WTs, there are three control actuators [5, 6]: pitch actuator, torque actuator and yaw actuator. Among them, the former two actuators are considered as the two dominating ones, since they can give a fast response that answers the rapid variation of wind speed. Up to date, there are large quantities of literature that focus on control methods for the pitch actuator and torque actuator. By comparison, the literature about the yaw system control is limited. Nevertheless, the function of the yaw system should not be overlooked.

Performance of yaw system may affect performance of the WT. On one side, a yaw misalignment may lead to a decreased power capture. Theoretically, the captured power is deceased by the cube of the yaw error. Although empirical data have shown that the relationship could be cosine-squared instead of cosine-cubed [7,8], it is obvious that the yaw misalignment results in the power reduction of the WT. On the other side, a yaw misalignment may bring about an increase of component loads. In a study of Schepers [9], he conducted a comparison investigation between calculations and measurements on a small WT with 10[m] rotor diameter in yaw, which revealed that the yaw misalignment had effects on blade root and shaft loads on a sectional level.

Boorsma in [10] presented a data report of power production and component loads for a 2.5[MW] WT in yawed flow conditions, in which the edgewise fatigue equivalent

Manuscript received May 18, 2017; accepted June 7, 2017. Recommended by Associate Editor Sun Jin Yoo under the direction of Editor Hyun-Seok Yang. This work is supported by the National Natural Science Foundation of China under Grant 51677194, the Project of Innovation-driven Plan in Central South University, the Program for New Century Excellent Talents in University under Grant NCET-13-0599, the Postdoctoral Science Foundation of Central South University, key scientific and technological plan of Hunan Province (2016GK2039), and the Basic Science Research Program through the National Research Foundation of Korea (NRF) funded by the Ministry of Education (NRF-2016R1A6A1A03013567) and Korea Electric Power Corporation (Grant number: R17XA05-17).

Dongran Song and Jian Yang are with the School of Information Science and Engineering, Central South University, Changsha 410083, P. R. China (e-mails: humble_szy@163.com, jian.yang@csu.edu.cn). Yao Liu is with Guangdong Power Grid Corp, Zhuhai Power Supply Bur, China (email: yaoliu@csu.edu.cn). Mei Su and Anfeng Liu are with the School of Information Science and Engineering, Central South University, Changsha 410083, P. R. China (e-mails: sumeicsu@csu.edu.cn, afengliu@mail.csu.edu.cn). Young Hoon Joo is with the Department of Control and Robotics Engineering, Kunsan National University, Kunsan, Chonbuk 573-701, Korea (e-mail: yhjoo@kunsan.ac.kr).
* Co-corresponding authors.

loads were found to be increased along with the increasing yaw error. From these data, it is obvious that the WT performance is indeed significantly determined by the yaw system. Therefore, the yaw control system should deserve more attentions.

The yaw control methods are mainly relevant to the measurement techniques [11]. In current industrial WTs, a typical yaw controller is comparably simple and activated when the yaw error that is measured by wind vanes mounted on the nacelle exceeds some thresholds. Although the control logic is simple, a qualified controller that can provide satisfactory performance is not easily implemented. The difficulty consists in obtaining a proper reference for adjusting the nacelle position. The yaw error measured by the wind vanes or sonic anemometers is noticeably disturbed by the WT operation. Therefore, an averaging filter is widely utilized to filter the measured yaw error and then used to provide the yawing movement reference. However, the filtered yaw error suffering from time delay is not the real yaw error. Meanwhile, the wind direction is changing all the same, thus the measured wind direction is different from the future wind direction. Studies of operating WTs revealed that a static yaw error of 10 degree for wind speeds below 20[m/s] and 5 degree for wind speeds above 20[m/s] [12]. Besides, statistical data regarding the failure rate and downtime of WTs showed that the portion of downtime caused by yaw system failure comprised 13.3% of the total downtime, and the yaw system failure rate comprised 12.5% [13, 14]. Consequently, yaw control methods based on measured wind direction provide general performance but needs to be optimized.

Recently, there has been growing interest in how the yaw controls can be improved. Some solutions for improving the yaw alignment using advanced measurement devices have been addressed in the literature [15–17]. From results of these studies, increased energy production due to the improved measurement system has been observed. Nevertheless, the proposed solutions required additional measurement devices that brought a high cost, thus these solutions were only employed in researching projects. For convenience of industrial applications, the prediction technology may be an alternative method. In the past years, there have been a large number of studies that investigated different prediction approaches for wind speed [18–20]. By comparison, studies about wind direction prediction are limited, among which wind direction was predicted along with the wind speed. For example, Yang *et al* predicted wind speed, wind direction and ambient temperature by using Bayesian approach [21]; Ergin *et al* computed wind direction and wind speed based on predicted values of lateral and longitudinal components of wind speed [22]. Besides, Ouyang *et al* proposed a time-series model for predicting wind direction [23] and Sheibat-Othman *et al* estimated a yaw error by support vector machines [24]. Although above studies addressed the issue of wind direction prediction, these prediction models were developed using data at 10 min or 1h intervals. Besides, these data are instantaneous values rather than mean values. Accordingly, the developed prediction models may be unsuitable for yaw control of WTs.

Motivated by the aforementioned studies, in this paper, we present a big gap between the need of wind energy industry and academic research in prediction methods. The objective of this study aims at bridging this gap. To do so, two prediction methods for the wind direction are developed and investigated. The first method adopts a classical time-series ARIMA (auto-regressive integrated moving average) prediction model, and the second one uses a hybrid model that integrated the ARIMA model into a Kalman filter (KF). Considering the practical need of the yaw control method, three types of wind direction data averaged in different periods are firstly derived to build the statistical ARIMA models. After that, the ARIMA models are integrated into the KF and formed ARIMA-KF hybrid models. Finally, performance of the developed prediction models are investigated and compared through some simulations.

The remainder of this work is organized as follows: the wind direction measurement and a typical yaw control algorithm are introduced in Section 2; and Section 3 describes the two wind direction prediction methods. This is followed by prediction results discussions in Section 4. Finally, conclusions are drawn in Section 5.

2. YAW CONTROL ALGORITHM AND WIND DIRECTION MEASUREMENT

2.1. Yaw control algorithm

In this study, the yaw control algorithm for WTs manufactured by China Ming Yang Wind Power (CMYWP) is introduced. The control algorithm is illustrated in Fig. 1. The yaw error that is the difference between the wind direction and the nacelle position of the WT, is measured by the wind vane mounted on the rear of the nacelle. This error is averaged by three averaged units with different averaged period. When one of the averaged values is larger than the predefined threshold and lasts more than the predefined time threshold, the yaw system is activated and moves to the yaw set-point. The yaw set-point not given here is defined according to the output of averaged units.

From above discussions, it can be known that the presented yaw control algorithm depends entirely on the yaw error. Since the measured yaw error is easily disturbed by the WT's operation and accuracy of the measurement device, averaged calculation units are used to provide more reliable result. However, the averaged values only reflect past yaw error and result in a control delay. Therefore, it is reasonable to use prediction values to improve the performance of the yaw control system.

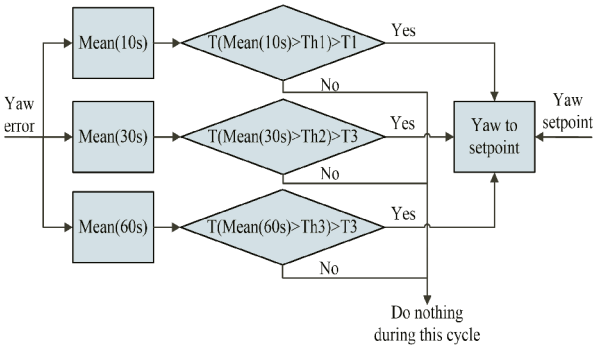

Fig. 1. Schematic of the yaw control algorithm for WTs of CMYWP.

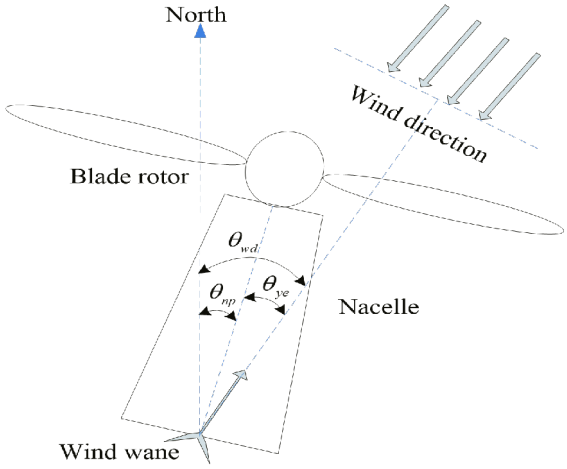

Fig. 2. Schematic of wind direction measurement.

2.2. Wind direction measurement

For an industrial WT, there are two types of transducers in yaw control system: one measures the nacelle position (θ_{np}) and the other measures the yaw error (θ_{ye}).

Fig. 2 shows the principle of wind direction measurements. From Fig. 2, it can be seen that wind direction (θ_{wd}) can be calculated by

$$\theta_{wd} = \theta_{np} + \theta_{ye}, \tag{1}$$

where $\theta_{ye} \in [0^\circ, 360^\circ]$, $\theta_{np} \in [-1080^\circ, 1080^\circ]$.

As clearly seen from (1), yaw error is the difference between the wind direction and nacelle position. Since the wind direction varies along with the time, the yaw control system is developed to adjust the nacelle position to track the direction. However, a fast movement of a yaw system will induce high component loads. Accordingly, the yaw speed for a large WT is normally designed in a range of $[0.2\,\mathrm{deg}/s, 0.8\,\mathrm{deg}/s]$. Meanwhile, to avoid over-usage of yaw driver, the yaw system is always activated at discrete intervals rather than continuous. As a consequence of the control delay, the yaw error is hard to eliminate. Obtaining wind direction prediction may be useful to provide a more reasonable reference for the yaw control system. Therefore, a decreased yaw error may be obtained and promote performance of the WT.

In addition, it is worthy noticing that θ_{wd} calculated by θ_{ye} and θ_{np} may be out of the range of $[0^\circ, 360^\circ]$. Therefore, θ_{wd}has to be scaled by some manipulations, which is not given here for sake of simplicity.

3. TWO PREDICTION METHODS

Prediction approaches discussed in the literature fall into two categories: physical models and statistical models. Physical models use multiple parameters, such as geographic conditions, temperature and pressure, to build multivariate forecasting models. It is good at obtaining long-term prediction results and has been applied in weather prediction. By comparison, statistical models employ mathematical equations to make prediction based on a number of historical data, among which the most notable approaches are the ARIMA-based models introduced by Box and Jenins [25]. Since the ARIMA-based models reproduce the patterns of the prior movements of a variable over time that are used to predict its future movements, it is an effective way to construct a simplified model of the time series that represents its randomness. Statistical methods often exhibit limited prediction accurateness, thus the post-processing approaches have been proposed to obtain better performance. In this study, we use two prediction methods for the wind direction prediction: one uses an ARIMA-based model, whereas the other one employs a hybrid ARIMA-KF model.

3.1. ARIMA-based prediction method

ARIMA models were popularized by Box and Jenins in the early 1970s. There are many ARIMA models and the typical one is known as non-seasonal model and can be denoted as $ARIMA(p,d,q)$, where:

AR: p =order of the auto-regression of the model;

I: d =order of differencing to make the model stationary;

MA: q =order of the moving average aspect of the model.

Above notations can be expressed as follows:

$$y_t = \sum_{i=1}^{p} \phi_i y_{t-i} + \sum_{j=1}^{q} \varphi_j e_{t-j} + e_t, \tag{2}$$

where y_t represents the value of wind direction observed or forecast at time t, $\phi_i$is the i-th auto-regressive coefficient, $\varphi_j$is the j-th moving-average coefficient, and $e_t$is the error term at time period t.

Building an ARIMA model is basically a three-step iterative step that includes:

1) Model identification. This first step determines suitable values for parameters p, q and the order of differenc-

ing, d. For this purpose, inspection of the run plots and auto correlation function (ACF) plots can be used for deciding d. P and d can be decided using ACF and the partial auto correlation function (PACF) plots.

2) Parameter estimation. After specifying an initial model, model parameters can be estimated from the maximum likelihood or conditional least squares methods.

3) Diagnostic checking. For the diagnostic checking properties, ACF and PACF graphs of the residuals are analyzed. If the model is good fit to the data, the residuals would correspond to white noise and have little autocorrelation.

3.2. KF-based prediction method

KF is the statistically optimal sequential estimation procedure for dynamic systems [26]. Observations are recursively combined with recent forecasts with weights that minimize the corresponding biases. The main advantage of this method is the easy adaption to any alteration of the observation and the fact that it needs short series of background information. Due to its good performance, it has been utilized in many application, such as in recent studies of us [27–29], KF was used to estimate the effective wind speed.

Based on the type of the target system, there are two types of KF algorithms: the linear KF algorithm and the nonlinear KF algorithm (or the extended KF algorithm). Since the linear ARIMA model is used in this study, the linear KF algorithm is applied here. The algorithm procedure is given as follows:

1) System modeling. The first step is to describe the system modeling equation in a standard form as

$$x(t+1) = Ax(t) + w(t+1), \tag{3a}$$
$$y(t+1) = Cx(t+1) + v(t+1), \tag{3b}$$

where $x(t+1)$ and $y(t+1)$ represents the state and measurement, respectively; $w(t+1)$ and $v(t+1)$ represents the state and measurement noises, respectively.

2) Measurement update. The measurement update is fulfilled by

$$x(t+1) = x(t+1/t) + K(t+1)(y(t+1) - Cx(t+1/t)), \tag{4a}$$
$$K(t+1) = P(t+1/t)C^T(CP(t+1/t)C^T + R(t+1))^{-1}, \tag{4b}$$
$$P(t+1) = (I - K(t+1)C)P(t+1/t), \tag{4c}$$

where $K(t+1)$ and $P(t+1)$ represents the Kalman gain and state estimation error covariance, respectively; $R(t+1)$ is the measurement noise covariance.

3) Time update filter gain. The time update is fulfilled by

$$x(t+2/t+1) = Ax(t+1), \tag{4d}$$

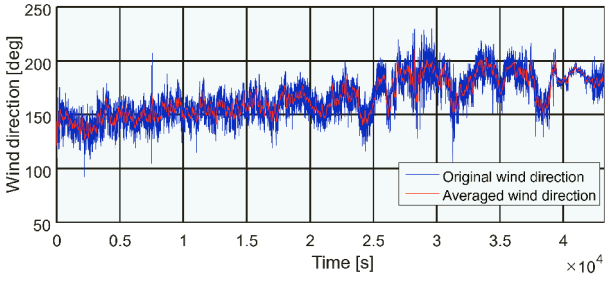

Fig. 3. Original wind direction and its averaged series.

$$P(t+2/t+1) = AP(t+1)A^T + Q(t+1), \tag{4e}$$

where $Q(t+1)$ is the state noise covariance.

4. MODEL DEVELOPMENT AND PREDICTION RESULTS

4.1. Wind direction data

The wind direction data in this paper was obtained from an operating wind farm that locates in Guangdong Province of China. Since the averaged wind direction is used for the yaw control system, the data collected at 1 second intervals was used to calculate averaged values with different periods. Three types of time series data are included: mean values in 10-second, 30-second and 60-second periods, respectively.

Fig. 3 shows a wind direction series in a half day (including 43200 seconds) and its mean values averaged in one minute period. The first 30000-second ones of those data are used to establish models, the leaving 13200 ones to check the model validity. As shown in Fig. 3, the original wind direction data is mixed with high-frequency noises, and the averaged values gave much smooth results. Besides, it can be seen that this section of data is non-stationary.

4.2. Model development

To illustrate the modeling development, the time series of one-minute averaged wind direction was used to establish the model. Other two models are developed in a similar way.

1) ARIMA-based prediction model

The ACF and PACF values for the first 30000-second series are displayed in Fig. 4. From Fig. 4, we obtained the data was non-stationary, since the PACF had a trailing character meanwhile the ACF had a slow decreasing phenomenon. Thus, the differencing approach was used. The differencing results and their ACF/PACF values are given in Fig. 5. From Fig. 5, we found out the wind direction series after the first difference met a low-order AR model, because the ACF decreased fast and the PACF showed a cutoff value after lag 2 or probably lag 4.

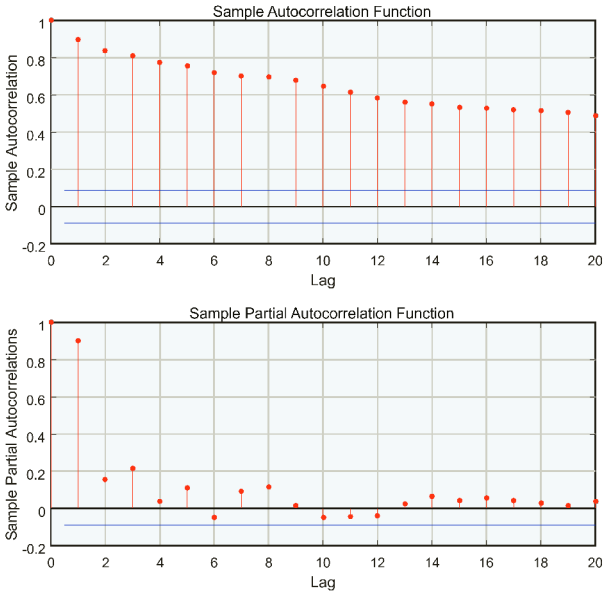

Fig. 4. ACF and PACF graphs for the original wind direction series.

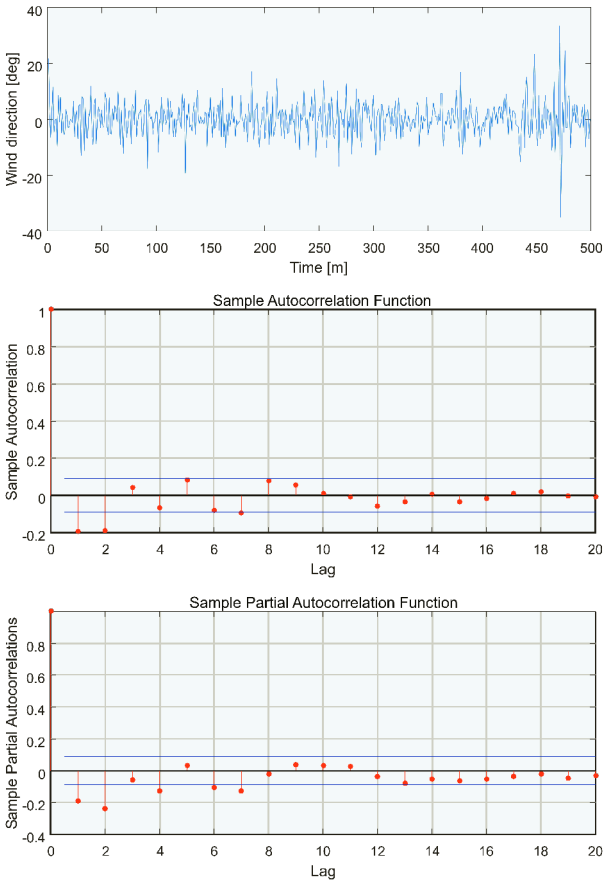

Fig. 5. Differencing results and their ACF and PACF graphs.

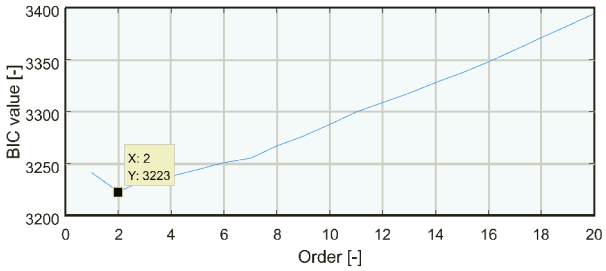

Fig. 6. BIC values for various ARIMA models.

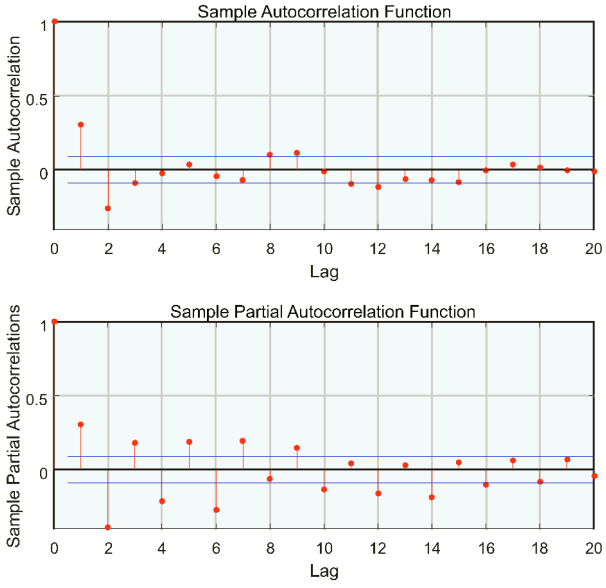

Fig. 7. ACF and PACF graphs for the residuals.

According to the patterns on ACF and PACF graphs, models with $ARIMA(2,1,0)$ and $ARIMA(4,1,0)$ are considered to be valid for this time series. To choose the best model order, the Bayesian Information Criterion (BIC) is used to specify the tentative orders for the auto-regressive and moving average [30–32]. The combination yielding the smallest BIC value is selected. Fig. 6 illustrates the corresponding BIC values for the various ARIMA models with auto-regressive orders varying from 1 to 20. It can be seen that the minimum BIC value is obtained with $ARIMA(2,1,0)$, which also supports the conclusion made based on Fig. 5.

Then, $ARIMA(2,1,0)$ model parameters are obtained through the least-squares estimation algorithm. The estimation procedure minimizes the sum of square of the residuals during a backward approach, where the values in time series are reversed and parameters are obtained based on the residuals of the fitted model. After that, ACF and PACF graphs of the residuals are analyzed and shown in Fig. 7, which reveal that there is no other pattern present in the residual.

Table 1. Model parameters for three time series.

Time series	Models
1	$y_t = -0.2456y_{t-1} - 0.2375y_{t-2} + e_t$
2	$y_t = -0.1463y_{t-1} - 0.1864y_{t-2} - 0.2y_{t-3} + e_t$
3	$y_t = -0.2795y_{t-1} - 0.1562y_{t-2} - 0.1y_{t-3} - 0.0779y_{t-4} + e_t$

Finally, the obtained model parameters are summarized in Table 1, where three time series models are provided. Time series 1, 2 and 3 represent 60-second, 30-second and 10-second averaged wind direction data.

2) ARIMA-KF hybrid prediction model

The key of utilizing KF method is to model the system in a standard form as given in (3a) and (3b). In this paper, the ARIMA model is used to provide the system modeling for a KF-based model.

The explicit equation of the $ARIMA(2,1,0)$ model in Table 1 is reformulated as

$$x_t = -0.2456x_{t-1} - 0.2375x_{t-2} + e_t. \tag{5}$$

Set:

$$x_i(t) = x_{t-i}, \quad (i = 1,2,...,20). \tag{6}$$

Then, we have

$$x_1(t+1) = -0.2456x_1(t) - 0.2375x_2(t) + e_t. \tag{7}$$

Set:

$$x_2(t+1) = x_1(t). \tag{8}$$

So, we obtain

$$\begin{bmatrix} x_1(t+1) \\ x_2(t+1) \end{bmatrix} = \begin{bmatrix} -0.2456 & -0.2375 \\ 1 & 0 \end{bmatrix} \times \begin{bmatrix} x_1(t) \\ x_2(t) \end{bmatrix} + \begin{bmatrix} 1 \\ 0 \end{bmatrix} \times e(t+1). \tag{9a}$$

The measurement equation can be expressed as

$$y(t+1) = [1\ 0] \times [x_1(t+1)\ x_2(t+1)]^T + v(t+1). \tag{9b}$$

After establishing the standard form model, the KF algorithm expressed in (4a)-(4e) is employed. Before that, the initial state and prediction covariances are chosen as $x(0) = [1\ 0]^T$ and $P(0) = [1\ 0;0\ 1]^T$, respectively; The process and measurement covariances are chosen as $Q = [10\ 0;0\ 10]^T$ and $R = 0.1$, respectively.

Other two hybrid ARIMA-KF models for time series 2 and 3 are developed in a similar way and not given here for sake of simplicity.

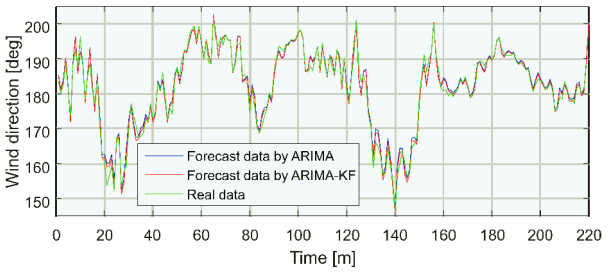

Fig. 8. Forecast data and real data in time series 1.

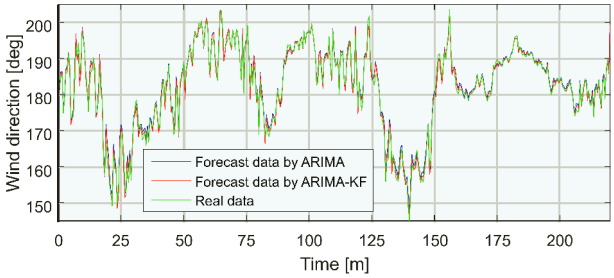

Fig. 9. Forecast data and real data in time series 2.

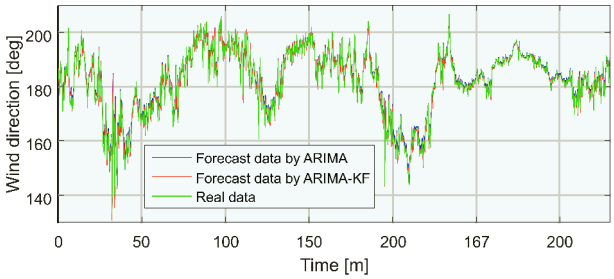

Fig. 10. Forecast data and real data in time series 3.

4.3. Prediction results

1) Time series results

In order to check performance of the two proposed prediction methods for forecasting different time series data, the prediction results by six prediction models are shown in Figs. 8-10. Figs. 8-10 show forecasting results of time series 1 with 60-second mean values, the ones of time series 2 with 30-second mean values and the ones time series 3 with 10-second mean values, respectively. From these three figures, we can see that there are only slightly difference among forecasting results and real results under different time series. Therefore, we can conclude that the developed prediction models by ARIMA and ARIMA-KF methods provide good performance for the concerned three time series.

Besides, the results forecast by ARIMA-KF models are slightly closer to the real data than the ones by the ARIMA models. To further verify this conclusion, statistical results are compared in the next subsection.

Table 2. Statistical results of forecast data shown in Figs. 8-10.

Indexes	ARIMA-KF			ARIMA		
	Series 1	Series 2	Series 3	Series 1	Series 2	Series 3
MAE	1.2432	0.9675	0.9384	1.333	1.0812	1.0754
MSE	2.7303	1.6812	1.7146	3.1981	2.055	2.1295
MAPE	12.44%	13.30%	16.83%	12.80%	13.48%	17.05%

2) Statistical results

To assess performance of the developed prediction models, three types of performance indexes are used to compare: mean absolute error (MAE), mean squared error (MSE) and mean absolute percentage error (MAPE). MAE is the mean of absolute values of the forecast errors, MSE is the mean of squared values of the forecast errors, and MAPE is the mean of absolute values of the forecast error percentages. Their calculations are expressed as

$$\begin{cases} MAE = \dfrac{1}{N}\sum_{t=1}^{N}|y_t - y_t'|, \\ MSE = \dfrac{1}{N}\sum_{t=1}^{N}(y_t - y_t')^2, \\ MAPE = \dfrac{1}{N}\sum_{t=1}^{N}|(y_t - y_t')/y_t| \times 100\%, \end{cases} \tag{10}$$

where y_t and y_t' are the real value and the forecast value at time period t, and N is the number of the data points.

Using (10), the statistical results by the ARIMA and ARIMA-KF prediction models are given in Table 2. From Table 2, it is very clear that all MAE, MSE and MAPE by ARIMA-KF models are smaller than those ones by ARIMA models. By comparison to the results by the ARIMA models, the ARIMA-KF models decreased the MAE about 6.73%, 10.51% and 12.74%, the MSE about 14.62%, 18.19% and 19.48%, the MAPE about 2.81%, 1.33% and 1.29%, for time series 1, 2 and 3, respectively. These statistical properties reveal that the hybrid ARIMA-KF prediction method outperform the ARIMA method.

In Table 2, another trend for the statistical results is pronounced, that is, when the averaged period is getting shorter from 60 seconds to 10 seconds, the MAE values are decreasing, and the MAPE values are increasing. This trend well agrees the results in Figs. 8-10. The real data in the 10-second mean time series shows a bigger variation than the one in the 60-second mean time series.

5. CONCLUSIONS AND FUTURE WORK

In this paper, two time series-based prediction methods have been proposed for wind direction prediction, that is, the ARIMA method and the hybrid ARIMA-KF one. Since the prediction values aim at application in yaw control, the mean values of wind direction data are used to establish the prediction models and three time series of wind direction mean values are considered. To introduce the model development, we discuss the ARIMA model and its corresponding ARIMA-KF model with the time series data of 60-second mean wind direction. Finally, we have demonstrated some prediction results and statistical results for the developed six prediction models by using industrial data. The results have shown that the developed prediction models can provide good forecast results. Meanwhile, better performance has been observed by the ARIMA-KF models than the ARIMA models. Therefore, it is shown that the hybrid model has a potential application into optimal yaw control for WTs.

Regarding the fact that the current yaw control method employed by industrial WTs entirely depends on the historical wind direction data, the control performance could be potentially improved by utilizing prediction information into the control rules. Our future work will be toward optimal yaw control method using the wind direction predictions.

REFERENCES

[1] Global Wind Energy Council, *Global Wind Statistics 2016*, Available online: http://www.gwec.net/wpcontent/uploads/vip/GWEC_PRstats2016_EN_WEB.pdf.

[2] S. Lindenberg, B. Smith, and K. O' Dell, *20% wind energy by 2030*, National renewable energy laboratory (NREL), US department of energy, renewable energy consulting services, energetics incorporated, 2008.

[3] National Development and Reform Commission, *"13th Five-Year" renewable energy development planning*, 2016.

[4] K. E. Johnson, L .Y. Pao, M. J. Balas, and L. J. Fingersh, "Control of variable-speed wind turbines: standard and adaptive techniques for maximizing energy capture," *IEEE Trans. Control Syst*, vol. 26, pp. 70–81, 2006. [click]

[5] X. S. Luo, "Data-driven predictive control for continuous-time linear parameter varying systems with application to wind turbine," *International Journal of Control Automation, and Systems*, vol. 15, no. 2, pp. 619-626, 2017. [click]

[6] L. Y. Pao and K. E. Johnson, "A tutorial on the dynamics and control of wind turbines and wind farms," *American Control Conference IEEE*, pp. 2076-2089, 2009.

[7] M. Spencer, K. Stol, and J. Cater, "Predictive yaw control of a 5MW wind turbine model," *AIAA Aerospace Sciences Meeting Including the New Horizons Forum and Aerospace Exposition*, 2013.

[8] K. A. Kragh and P. Fleming, "Rotor speed dependent yaw control of wind turbines based on empirical data," *AIAA Aerospace Sciences Meeting Including the New Horizons Forum and Aerospace Exposition*, 2012.

[9] J. G. Schepers, "Dynamic Inflow effects at fast pitching steps on a wind turbine placed in the NASA-Ames wind tunnel," *ECN Reports*, 2007.

[10] K. Boorsma, "Power and loads for yawed flow conditions," *ECN Reports*, 2012.

[11] F. A. Farret, L. L. Pfitscher, and D. P. Bernardon, "Sensorless active yaw control for wind turbines," *Industrial Electronics Society, 2001. IECON '01, the Conference of the IEEE*, vol. 2, pp. 1370-1375, 2001.

[12] M. S. Jeong, S. W. Kim, and I. Lee, "The impact of yaw error on aeroelastic characteristics of a horizontal axis wind turbine blade," *Renewable Energy*, vol. 60, no. 5, pp. 256-268, 2013. [click]

[13] J. Ribrant and L. M. Bertling, "Survey of failures in wind power systems with focus on Swedish wind power plants during 1997-2005," *IEEE Transactions on Energy Conversion*, vol. 22, no. 1, pp. 167-173, 2007. [click]

[14] J. M. P. Pérez, F. P. G. Márquez, A. Tobias, and *et al*, "Wind turbine reliability analysis," *Renewable & Sustainable Energy Reviews*, vol. 23, no. 23, pp. 463-472, 2013. [click]

[15] T. F. Pedersen, U. S. Paulsen, S. M. Pedersen, and *et al*, "operational experience and analysis of a spinner anemometer on a MW size wind turbine," 2008.

[16] K. A. Kragh, M. H. Hansen, and T. Mikkelsen, "Precision and shortcomings of yaw error estimation using spinner-based light detection and ranging," *Wind Energy*, vol. 16, no. 3, pp. 353-366, 2013. [click]

[17] E. Dakin, M. Priyavadan, and A. Hopkins, "Catching the wind - an update on improved yaw alignment," *Proceedings of EWEA*, 2011.

[18] A. K. Singh and S. Bhaumik, "Cubature quadrature Kalman filter," *International Journal of Control, Automation and Systems*, vol. 13, no. 5, pp. 1097-1105, 2015.

[19] P. E. Huang, Z. Y. Lu, and Z. X. Liu, "State estimation and parameter identification method for dual-rate system based on improved Kalman prediction," *International Journal of Control, Automation and Systems*, vol. 14, no. 4, 998-1004, 2016. [click]

[20] H. Liu, H. Q. Tian, and Y. F. Li, "Comparison of two new ARIMA-ANN and ARIMA-Kalman hybrid methods for wind speed prediction," *Appl Energy*, vol. 98, no. 1, pp. 415-424, 2012.

[21] M. Yang, S. Fan, and W. J. Lee, "Probabilistic short-term wind power forecast using componential sparse Bayesian Learning," *IEEE Transactions on Industry Applications*, vol. 49, no. 6, pp. 2783-2792, 2012. [click]

[22] E. Erdem and J. Shi, "ARMA based approaches for forecasting the tuple of wind speed and direction," *Appl Energy*, vol. 88, no. 4, pp. 1405-1414, 2011. [click]

[23] T. Ouyang, A. Kusiak, and Y. He, "Predictive model of yaw error in a wind turbine," *Energy*, vol. 123, pp. 119-130, 2017.

[24] N. Sheibat-Othman, R. Othman, R. Tayari, and *et al*, "Estimation of the wind turbine yaw error by support vector machines," *IFAC-Papers OnLine*, vol. 48, no. 30, pp. 339-344, 2015.

[25] G. E. P. Box, G. W. Jenkins, and G. C. Reinsel, *Time Series Analysis, Forecasting and Control*, 3rd ed., Prentice-Hall, Englewood Cliffs, USA, 1994.

[26] A. Gelb, J. F. Kasper, R. A. Nash, and C. F. Price, *Sutherland AA. Applied Optimal Estimation*, The M.I.T. Press, London, England, 1974.

[27] D. R. Song, J. Yang, M. Dong, and Y. H. Joo, "Kalman filter-based wind speed estimation for wind turbine control," *International Journal of Control, Automation and Systems*, vol. 15, no. 3, 1089-1096, 2017. [click]

[28] D. R. Song, J. Yang, Z. L. Cai, M. Dong, M. Su, and Y. H. Wang, "Wind estimation with a non-standard extended Kalman filter and its application on maximum power extraction for variable speed wind turbines," *Appl Energy*, vol. 190, pp. 670-85, 2017.

[29] D. R. Song, J. Yang, M. Dong, and Y. H. Joo, "Model predictive control with finite control set for variable-speed wind turbines," *Energy*, vol. 126, pp. 564-572, 2017.

[30] L. Ljung, *System Identification: Theory for the User*, Prentice-Hall PTR, Upper Saddle River, NJ, 1999.

[31] X. Liu, A. F. Liu, Z. T. Li, and et al, "Distributed cooperative communication nodes control and optimization reliability for resource-constrained WSNs," *Neurocomputing*, in Press, 2017. DOI: 10.1016/j.neucom.2016.12.105

[32] T Li, M. Zhao, A. F. Liu, and et al, "On Selecting Vehicles as Recommenders for Vehicular Social Networks," *IEEE Access*, vol. 5, pp. 5539-5555, 2017.

Dongran Song received the B.S., M.S. and Ph.D. degrees from the School of Information Science and Engineering, Central South University, Changsha, China, in 2006, 2009 and 2016, respectively, where he is currently working as a post-doctoral member. He was an Electrical & Control Engineer with China Ming Yang Wind Power, Zhongshan, from 2009 to 2016. His research interests include advanced control algorithms for wind turbines, power electronics and renewable energy system.

Jian Yang received the Ph.D. degree in Electrical Engineering from the University of Central Florida, Orlando, in 2008. He was a Senior Electrical Engineer with Delta Tau Data Systems, Inc., Los Angeles, CA, from 2007 to 2010. Since 2011, he has been with Central South University, Changsha, China, where he is currently an Associate Chair Professor with the School of Information Science and Engineering. His main research interests include control application, motion planning, and power electronics.

Yao Liu received the B.S. and M.S. degrees from the Central South University, Changsha, China, in 2011 and 2014, respectively. From 2014, he has been with Guangdong Power Grid Corp, Zhuhai Power Supply Bur. His research interests include renewable energy systems, distributed generation, and microgrid.

Mei Su received the B.S., M.S. and Ph.D. degrees from the School of Information Science and Engineering, Central South University, Changsha, China, in 1989, 1992 and 2005, respectively. Since 2006, she has been a professor with the School of Information Science and Engineering, Central South University. Her research interests include matrix converter, adjustable speed drives, and wind energy conversion systems.

Anfeng Liu received the M.S. and Ph.D. degrees from the School of Information Science and Engineering, Central South University, Changsha, China, in 2002 and 2005, respectively; where he is a professor. He is also a Member (E200012141M) of China Computer Federation. His major research interest is wireless sensor network and wind energy conversion systems.

Young Hoon Joo received the B.S., M.S., and Ph.D. degrees in Electrical Engineering from Yonsei University, Seoul, Korea, in 1982, 1984, and 1995, respectively. He worked with Samsung Electronics Company, Seoul, Korea, from 1986 to 1995, as a project manager. He was with the University of Houston, Houston, TX, from 1998 to 1999, as a visiting professor in the Department of Electrical and Computer Engineering. He is currently a professor in the Department of Control and Robotics Engineering, Kunsan National University, Korea. His major interest is mainly in the field of intelligent control, intelligent robot, human-robot interaction, wind-farm control, power system stabilization, and intelligent surveillance systems. He severed as President for Korea Institute of Intelligent Systems (KIIS) (2008-2009) and is serving as the Editor-in-Chief for the International Journal of Control, Automation, and Systems (IJCAS) (2014-present) and the Vice-President for the Korean Institute of Electrical Engineers (KIEE) (2013-present) and for Institute of Control, Robotics, and Systems (ICROS) (2016-present). Also, he is serving as Director of Research Center of Wind Energy Systems funded by Korean Government (2016-present).